

Wind Tunnel Test of a Full-Scale Heliostat

S. G. Peglow

Prepared by Sandia Laboratories, Albuquerque, New Mexico 87115
and Livermore, California 94550 for the United States Department
of Energy under Contract DE-AC04-76DP00789.

Printed June 1979

***When printing a copy of any digitized SAND
Report, you are required to update the
markings to current standards.***



Sandia Laboratories

Issued by Sandia Laboratories, operated for the United States Department of Energy by Sandia Corporation.

NOTICE

This report was prepared as an account of work sponsored by the United States Government. Neither the United States nor the United States Department of Energy, nor any of their employees, nor any of their contractors, subcontractors, or their employees, makes any warranty, express or implied, or assumes any legal liability or responsibility for the accuracy, completeness or usefulness of any information, apparatus, product or process disclosed, or represents that its use would not infringe privately owned rights.

Printed in the United States of America
Available from
National Technical Information Service
U. S. Department of Commerce
5285 Port Royal Road
Springfield, VA 22161
Price: Printed Copy \$4.00 ; Microfiche \$3.00

WIND TUNNEL TEST OF A FULL-SCALE HELIOSTAT

S. G. Peglow
Sandia Laboratories, Livermore

ABSTRACT

This report describes the wind tunnel tests performed in the NASA facility in December 1978 on a DOE prototype heliostat and presents a comparison of the data with analytically derived results. Testing consisted of obtaining loads, moments, dynamic behavior (via servo accelerometers) and flow visualization for the entire range of operational and survival configurations. The data from the test has been used to augment the significant analytical and experimental work done by the various contractors and Sandia in support of heliostat design and development.

CONTENTS

	<u>Page</u>
Introduction	9
Test Description	10
Instrumentation	13
Results	14
Summary and Conclusions	18
References	19

ILLUSTRATIONS

<u>Figure</u>		<u>Page</u>
1.	General Arrangement of the Ames 40- by 80-Foot Wind Tunnel Test Section and Shop Area	10, 11
2.	Strut Support in NASA Tunnel	12
3.	DOE Prototype Heliostat	12
4.	Proof Tests at the SLL Heliostat Development Laboratory	13
5.	Elevation Drive Proof Test	14
6.	Coordinate System for Forces and Moments	15
7.	Lift Versus Angle of Attack	15
8.	Drag Versus Angle of Attack	16
9.	Base Moment Versus Angle of Attack, 0° Azimuth	17
10.	Base Moment Versus Angle of Attack, 180° Azimuth	17

WIND TUNNEL TEST OF A FULL-SCALE HELIOSTAT

S. G. Peglow
Sandia Laboratories, Livermore

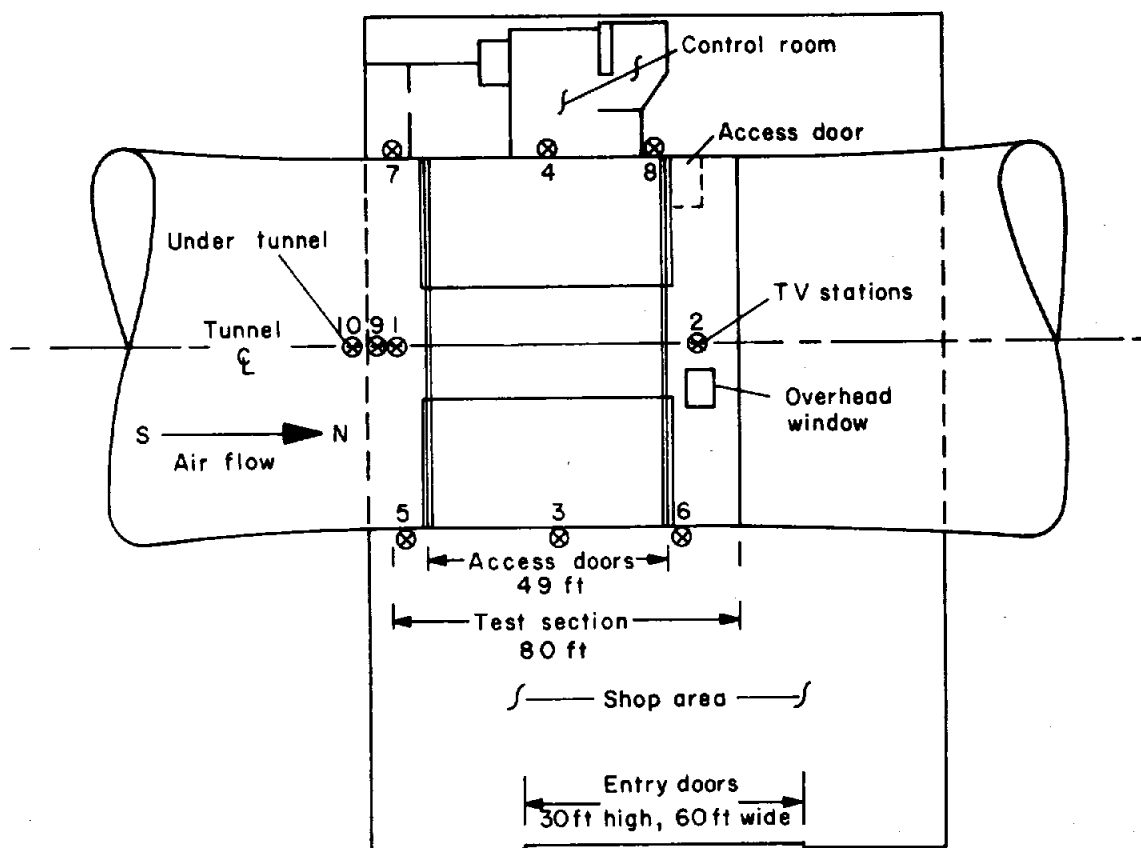
Introduction

To build a heliostat that will operate in and survive the extremes of weather conditions at a typical desert site, the designer must be able to predict the forces expected to act on the structure. To underestimate the design loads is to invite failure and to overestimate will invariably lead to a more costly heliostat.

The information needed to design or evaluate a heliostat for a wind environment consists of several elements. First, the environment must be characterized as well as meteorological data will allow. This has been done, for example, at the 10-MW pilot plant site located near Barstow, California. This has led to the establishment of a wind specification that calls for a maximum operational velocity of 50 mph (including gusts) and a maximum survival velocity of 90 mph (including gusts). Both of these conditions are assumed to occur at a height of 30 ft., with a velocity profile of the form $V = V_{30} (Z/30)^{0.15}$ to be used for values of Z other than 30 ft. Secondly, the loads and moments, both static and dynamic, acting on the structure must be calculated to allow evaluation of the capabilities of the drive mechanism and structure to provide reliable operation of the heliostat for the specified wind environment. The performance of these calculations implies a knowledge of the aerodynamic coefficients associated with a heliostat structure. Significant analytical and experimental work has been done in investigating the flow of air around bluff bodies and flat plates in two dimensions. Little data, however, is available for complex, three-dimensional flows at the large Reynolds numbers characteristic of a heliostat in a natural environment. It is to this end that a full-scale wind tunnel test of a DOE prototype heliostat was conducted.

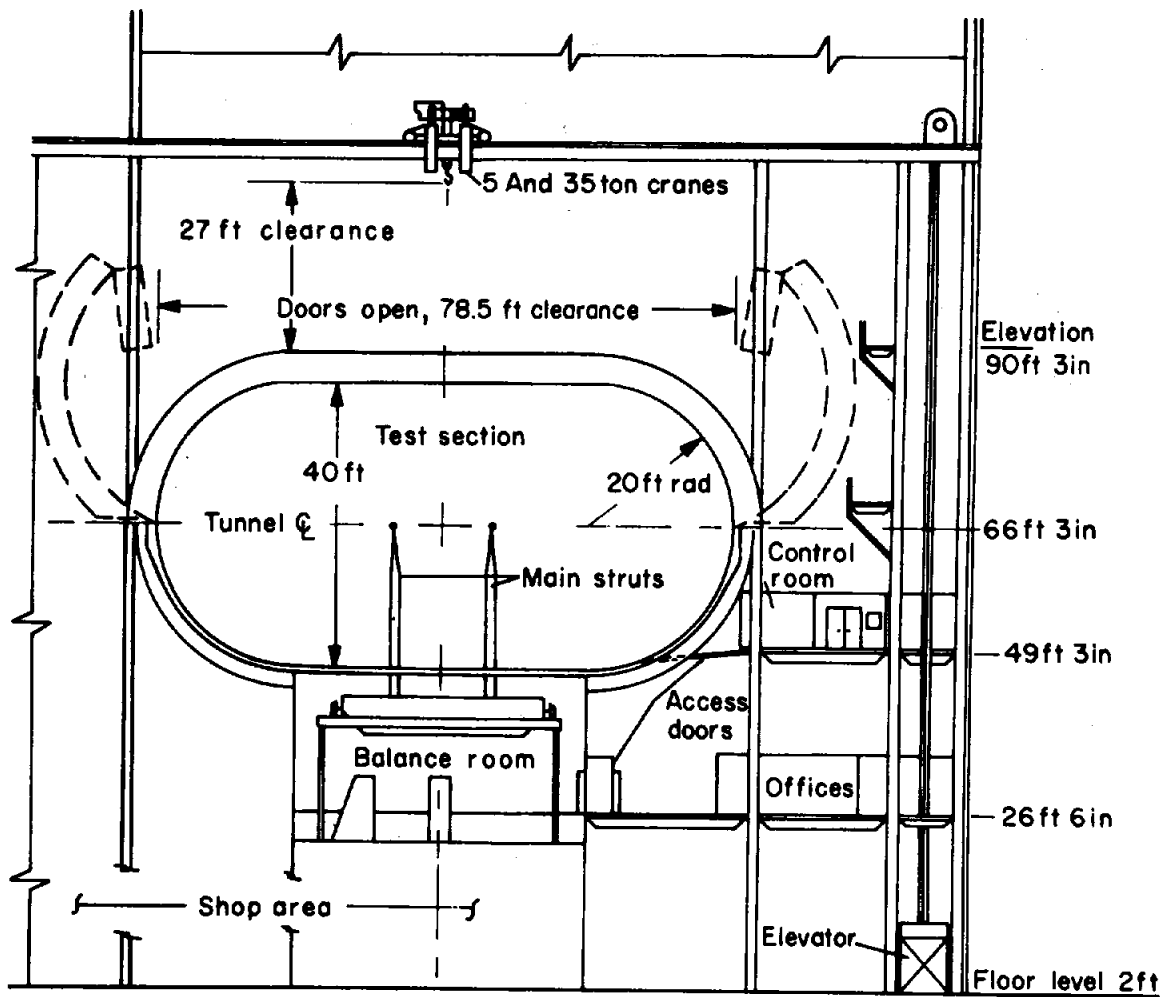
Test Description

The NASA, Ames, wind tunnel used in these tests has a closed 40- by 80-ft test section with semi-circular sides of 20-ft radius and a closed circuit air return as shown in Figure 1. The model support system consists of three movable struts mounted on a turntable. The heliostat was mounted on a single strut support as shown in Figure 2. Each strut is separately connected to the balance frame system. Mechanical lever systems transmit the lift, drag, and side force link loads to seven separate scales for measurement of loads and moments.



(a) Plan view.

Figure 1. General Arrangement of the Ames 40- by 80-Foot Wind Tunnel Test Section and Shop Area



(b) Elevation view.

Figure 1. (Continued)

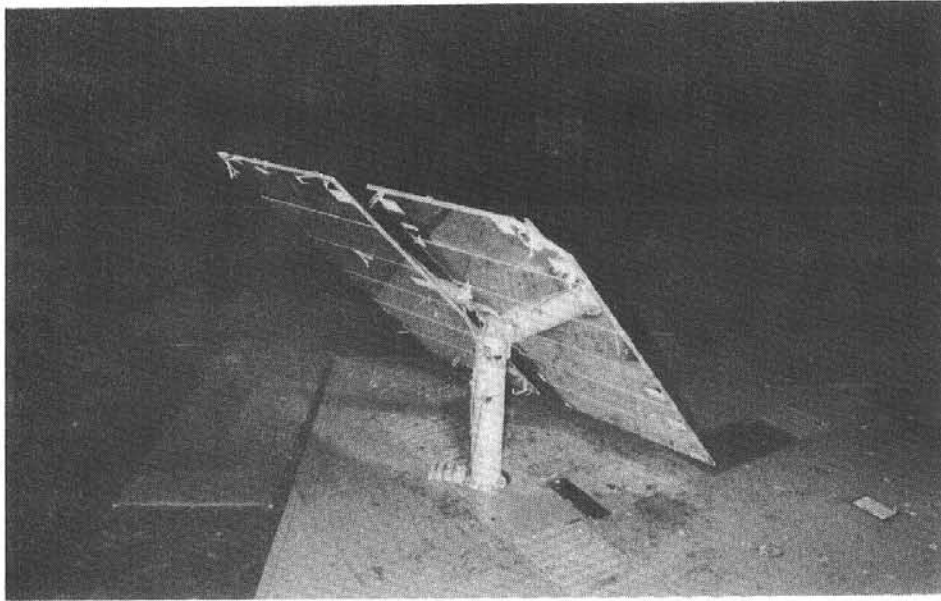


Figure 2. Strut Support in NASA Tunnel

The heliostat used in these tests was of the single pedestal, orbi-drive type built by McDonnell Douglas Astronautics for the DOE's prototype heliostat evaluation (Figure 3). The heliostat assembly consists of a galvanized steel pedestal supporting a torque tube to which are attached 8 frame arms and 12 mirror modules (402 ft² of reflective area). Movement of the mirror assembly is provided by two DC motors, one for elevation and one for azimuth, acting through separate gear boxes. During the tests, azimuth and elevation angle were changed by using the onboard drive motors and set by comparing potentiometer outputs to a list of precoded settings, which were verified by an inclinometer.

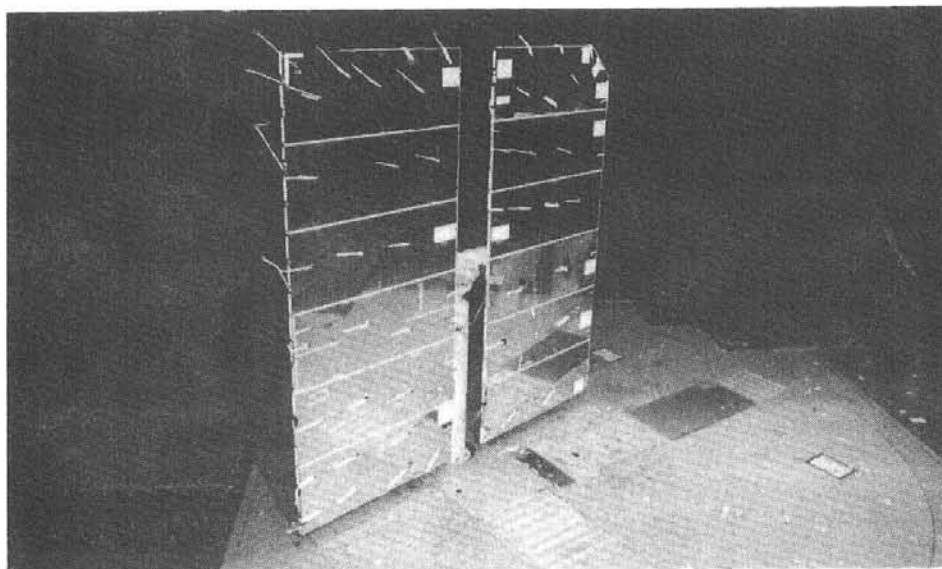


Figure 3. DOE Prototype Heliostat

Instrumentation

In addition to the force and moment data provided by the NASA balance system, twenty-six accelerometers were placed on the heliostat as defined in Reference 4. The type used were Sunstrand 3038 servo accelerometers with the gains in the amplifiers set to produce an output of ± 3.2 g's or ± 1.6 g's full scale depending on position. Several "shake" tests were run initially to establish the natural frequencies of the heliostat. As a more heuristic approach to the study of wind effects, strips of material were attached to the flow surfaces and the heliostat edges were Scotch-lited as shown in Figure 4. Both stills (Nikon at 3 frames/s) and 16-mm movies were used to capture the flow patterns on the heliostat surfaces for a variety of velocities and configurations.

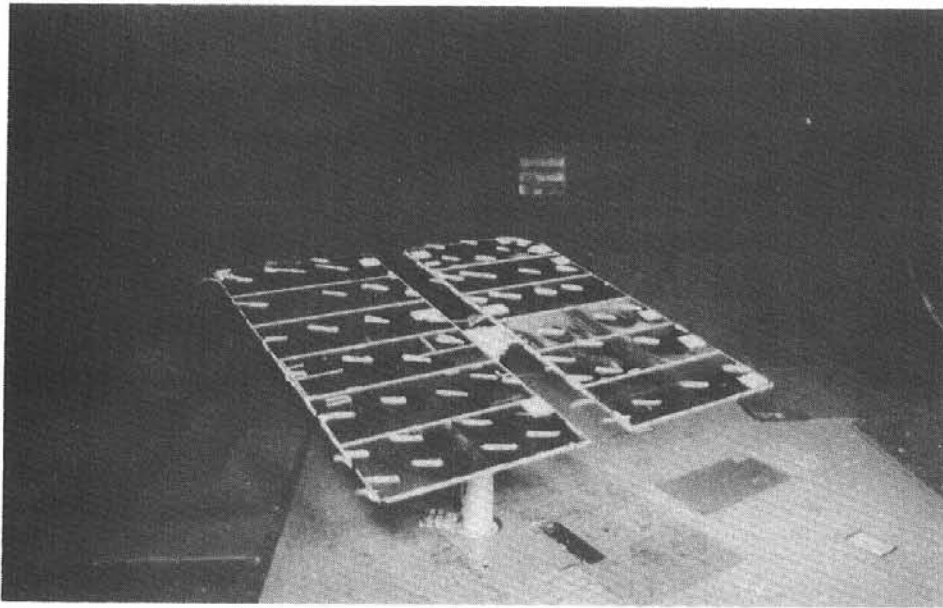


Figure 4. Flow Visualization

Proof Tests at the SLL Heliostat Development Laboratory

Prior to the NASA test, the prototype heliostat was subjected to a series of tests in which the 90-mph survival loads were applied to the heliostat mechanically as shown in Figure 5. The points of action were chosen so as to simulate the maximum torque about the elevation drive. Deflections of the frame arms were measured to evaluate the relative importance of dynamic deflections during the subsequent wind tunnel tests. The results are discussed in the next section and summarized in Table I. All accelerometers were first calibrated during static and shake tests and then checked at the NASA facility.

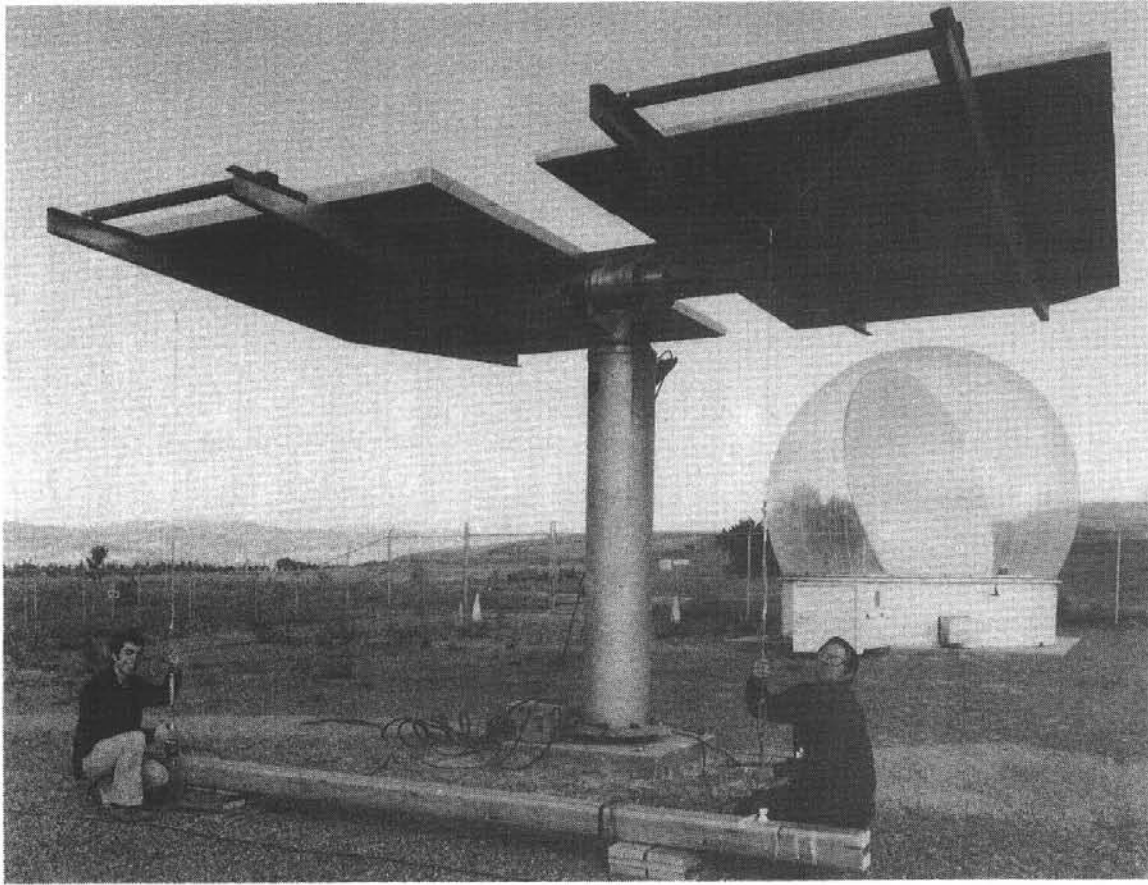


Figure 5. Elevation Drive Proof Test

Results

The force and moment data was taken at a point at the base of the heliostat as shown in Figure 6. The normal sense of lift and drag apply here, i.e., drag is positive down the tunnel and lift is positive upwards. In Figure 7, the lift force coefficient C_L is shown as a function of angle of attack (elevation), where positive α is opposite to the rotation shown for positive pitching moment and positive azimuth angle β is in the same direction as shown for positive yaw moment. This somewhat unorthodox choice of positive angular displacement is a result of control singularities when trying to rotate through the full range of angles required in the normal counterclockwise direction. The other data presented on the plot is the result of using data from the American Society of Civil Engineers, ASCE Paper No. 3269 and applying it to the prototype heliostat. Figure 8 shows the drag coefficient versus angle of attack. It is interesting to note that as the heliostat begins to approach a bluff body configuration, the total drag is best represented by assuming that the contribution from the mirror modules is approximated by two flat plates of aspect ratio λ equal to 3. The effect of the center slot is thus more noticeable at higher angles of attack.

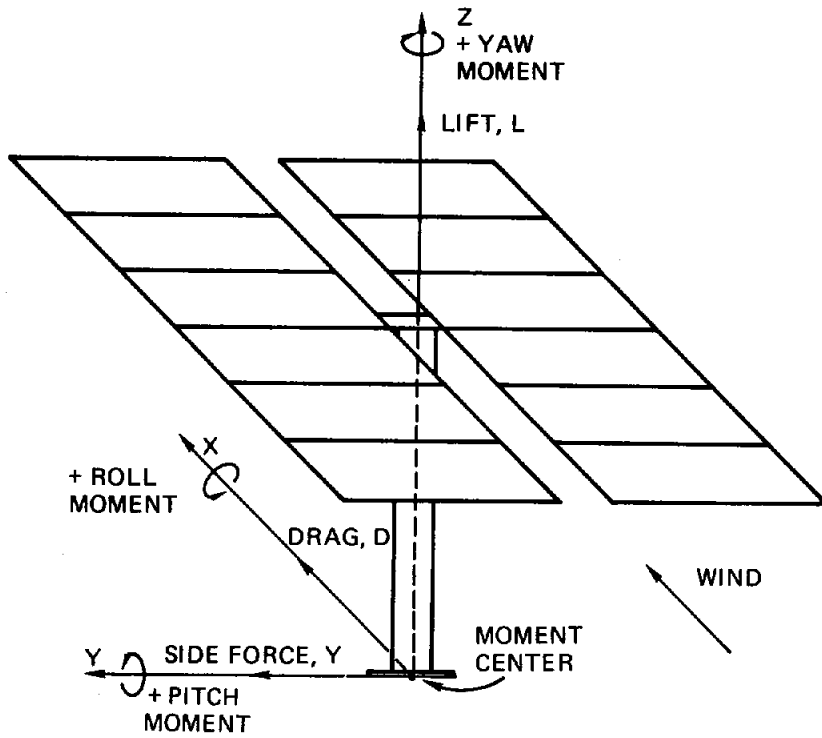


Figure 6. Coordinate System for Forces and Moments

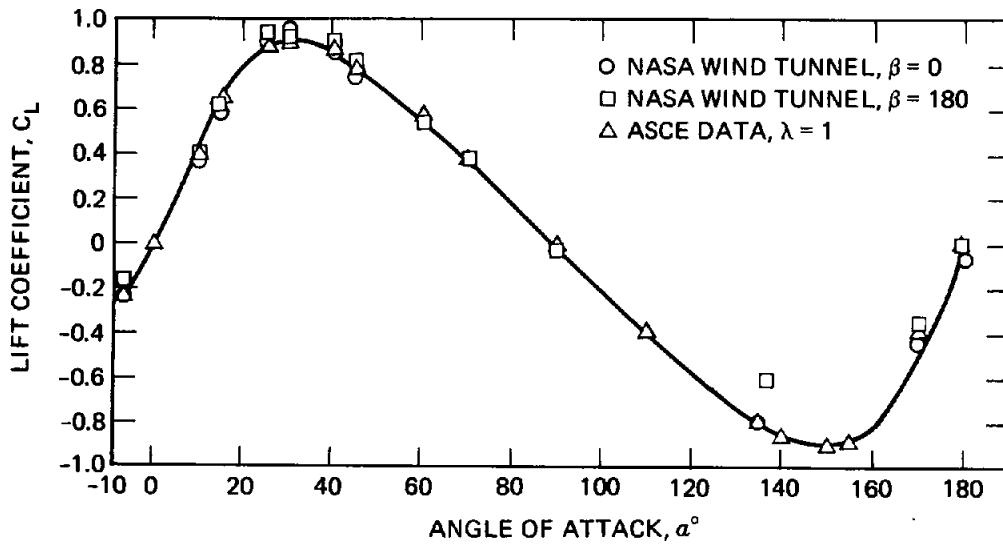


Figure 7. Lift Versus Angle of Attack

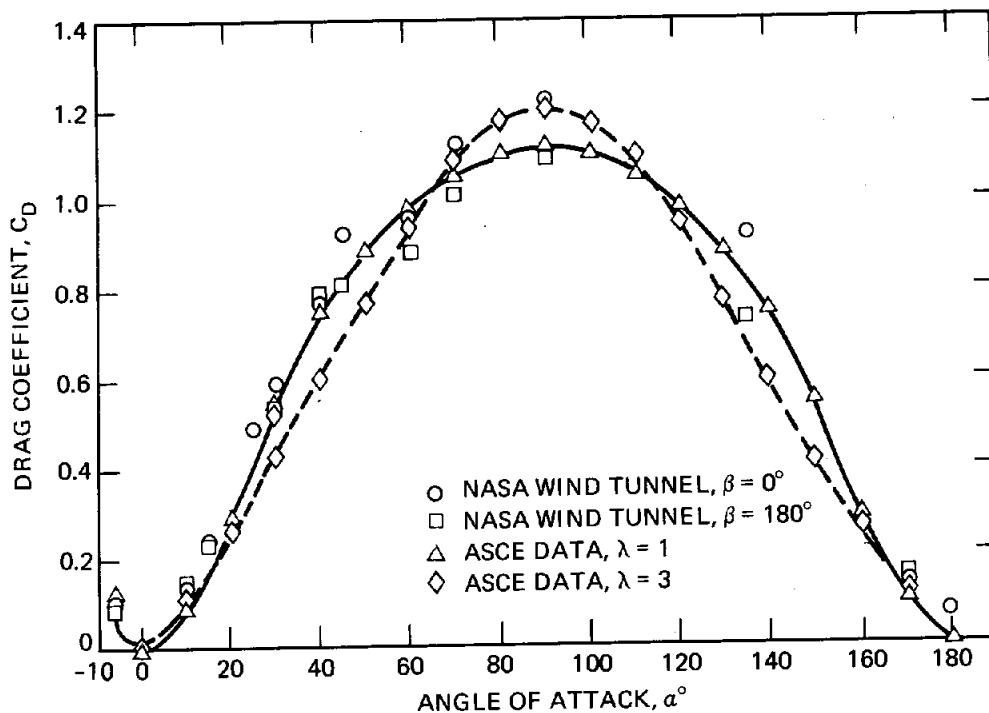


Figure 8. Drag Versus Angle of Attack

The variation of the base moment coefficient C_m with α is shown in Figures 9 and 10. With the glass side towards the flow, as shown in Figure 10, the pitch moment can be closely approximated by the flat plate data. With the structural side windward, however, the effect of the additional turbulence generated by the frame arms can be seen in the range of α from 25 degrees to 45 degrees where the maximum lift is occurring.

The dynamic loads on the heliostat structure were analyzed by taking the recorded real-time outputs of the twenty-six accelerometers mounted on the torque tube, frame arms, and pedestal and integrating the signals to produce power spectral density (PSD) plots. The worst vibration case during the tests was for the survival condition when the elevation angle was 10 degrees, the wind speed was 83 mph, and the azimuth angle was 45 degrees. The outboard panels downstream appeared to receive the worst buffeting effect in this configuration, which is verified by the accelerometer data. The accelerometer showing the highest vibration level yielded a PSD curve which has a pronounced peak of 0.04 g/Hz^2 at a frequency of 12 Hz. This corresponded to a real-time acceleration of $\pm 1.5 \text{ g's}$, which implies a dynamic displacement of less than 0.20 inches. As shown in Table I, the mechanically induced static displacements are greater than this dynamic value by more than an order of magnitude.

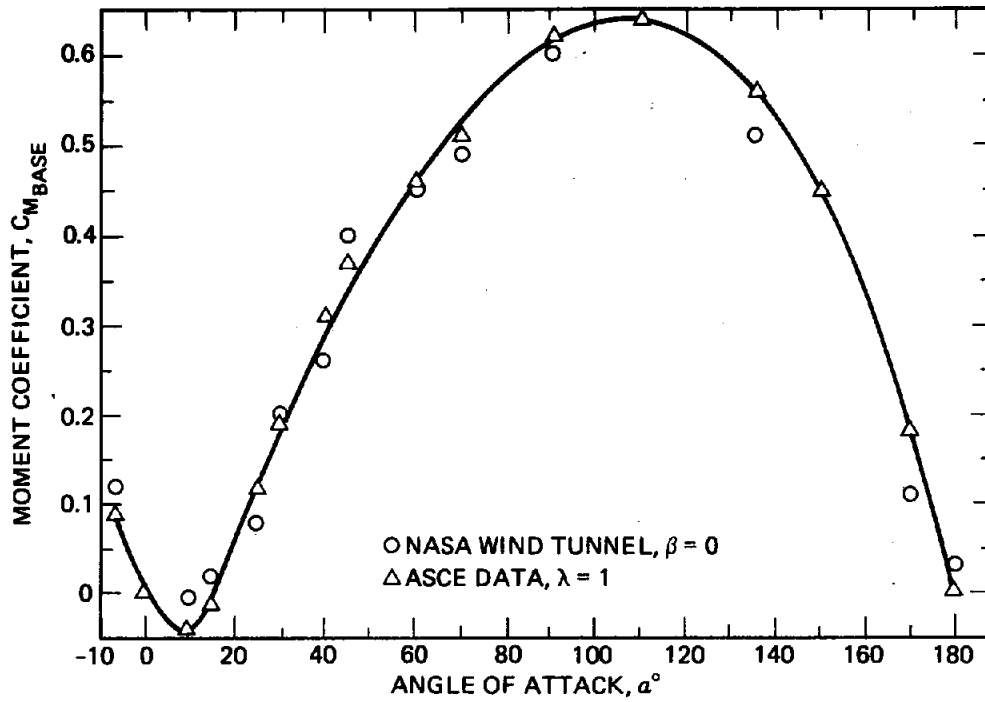


Figure 9. Base Moment Versus Angle of Attack, 0° Azimuth

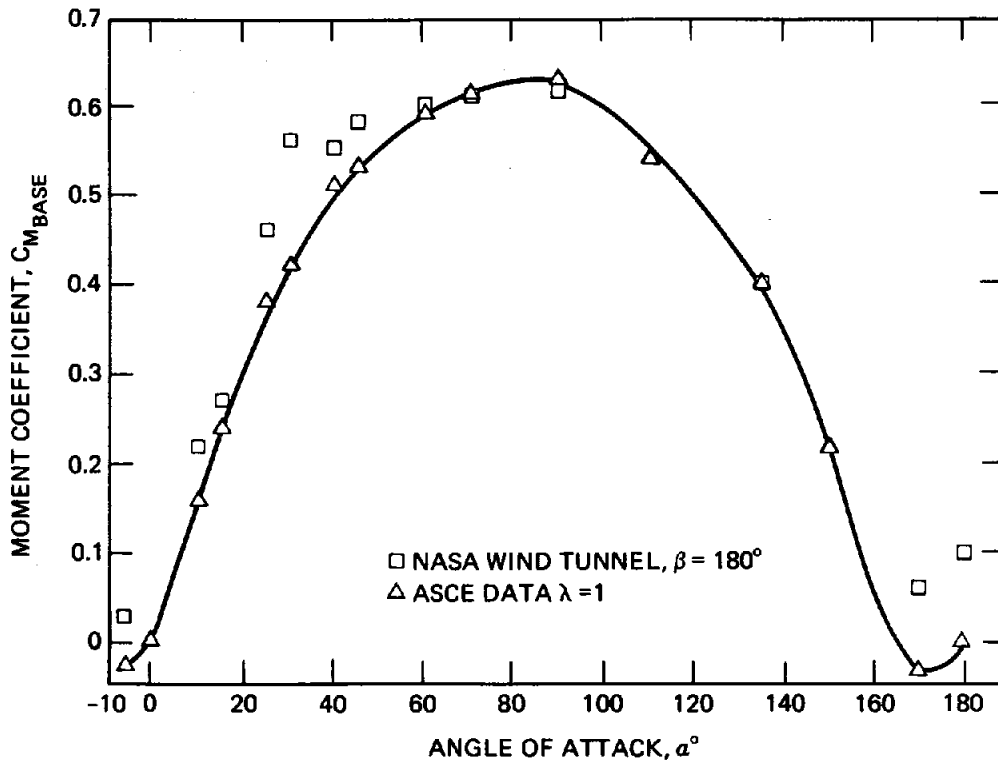


Figure 10. Base Moment Versus Angle of Attack, 180° Azimuth

TABLE I
STRUCTURAL DEFLECTION IN SIMULATED 90 mph WIND

Mechanically Applied Load
(195,000 in-lb about elevation drive)

<u>Test No.</u>	<u>Deflection (in.)</u>
1	3.15
2	3.24
3	3.26

Summary and Conclusions

The full-scale test of a DOE prototype heliostat in the NASA, Ames, 40- by 80-foot facility showed no severe airflow/structure dynamic interactions, such as low frequency vortex shedding. The heliostat survived the full range of configurations and wind speeds currently specified for heliostat design with no damage to any of the components. The results from this test indicate that the data and methodology defined in Reference 1 is appropriate for designing structures of this type. The proof tests outlined in this report would appear to be a valid way of mechanically simulating a survival moment about the critical elements (elevation or azimuth drive) to test future heliostats.

References

1. ASCE Paper No. 3269, "Wind Forces on Structures," Transactions, ASCE, Vol. 126, 1962.
2. "American Standard Building Code Requirements for Minimum Design Loads in Buildings and Other Structures," American National Standards Institute, 1971.
3. "Building to Resist the Effect of Wind, Vol. II," National Bureau of Standards, PB-266 333, May 1977.
4. Peglow, S. G., "Full Scale Heliostat Wind Tunnel Test Plan," Unpublished report, November 1978.

UNLIMITED RELEASE

INITIAL DISTRIBUTION:

TIC/UC62c (301)

U.S. Department of Energy (5)

6th and E Streets

Washington, D.C. 20545

Attn: M. Gutsein

G. Braun

G. Kaplan

L. Melamed

J. Weisiger

DOE/STMPO (2)

9550 Flair Drive, Suite 210

El Monte, CA 91731

Attn: C. Pignolet

Solar Energy Research Institute (2)

1536 Cole Boulevard

Golden, CO 80401

Attn: B. Butler

The Environmental Fund

1302 Eighteenth St., N. W.

Washington, D.C. 20036

Attn: W. Prichett

MIT-Lincoln Laboratory

Box 73, I-213

Lexington, MA 02173

Attn: Philip Jarvinen

BDM Corporation

2600 Yale Boulevard, S. E.

Albuquerque, NM 87106

Attn: A. Fong

Progress Industries, Inc.

7290 Murdy Circle

Huntington Beach, CA 92647

Attn: K. Busche

McDonnell Douglas Astronautics (3)

5301 Bolsa Ave.

Huntington Beach, CA 92647

Attn: J. Dietrich

J. Vaughn

J. Xerikos

Martin Marietta Corporation (2)
Denver Division
P. O. Box 179
Denver, CO 80201
Attn: R. Englund

Boeing Engineering and Construction Co. (2)
P. O. Box 3707
Seattle, WA 98124
Attn: R. Gillette

Northrup Inc. (2)
302 Nichols Drive
Hutchins, TX 75141
Attn: J. McDowell
J. Pletsch

Solaramics
1301 East El Segundo Blvd.
El Segundo, CA 90245
Attn: W. Mitchell

Westinghouse Electric Corporation
P. O. Box 10864
Pittsburgh, PA 15236
Attn: R. Devlin

Jet Propulsion Laboratory
MS-15 7316
4800 Oak Grove Drive
Pasadena, CA 91103
Attn: J. Roshke

Dept. Of Mechanical Engineering
Texas Tech University
Lubbock, TX 79409
Attn: J. Strickland

Accurex Corporation
485 Clyde
Mountain View, CA 94042
Attn: V. Wong

G. E. Brandvold, 4710; Attn: B. W. Marshall, 4713
R. P. Stromberg, 4714

D. L. King, 4713
R. H. Braasch, 4715
V. L. Dugan, 4720; Attn: J. V. Otts, 4721
J. F. Banas, 4722

J. R. Koterak, 5523
J. H. Scott, 5700
T. B. Cook, 8000; Attn: A. N. Blackwell, 8200
B. F. Murphey, 8300
L. Gutierrez, 8400; Attn: R. A. Baroody, 8410
C. S. Selvage, 8420
D. E. Gregson, 8440
C. M. Tapp, 8460

R. C. Wayne, 8450
W. R. Delameter, 8451
C. L. Mavis, 8451
S. G. Peglow, 8451 (10)
W. G. Wilson, 8451
A. C. Skinroad, 8452
J. D. Gilson, 8453
F. J. Cupps, 8265/Technical Library Processes Division, 3141
Technical Library Processes Division, 3141 (2)
Library and Security Classification Division, 8266-2 (3)